Journal of Applied Electrochemistry **29**: 869–881, 1999.

Influence of initial surface condition of lithium metal anodes on surface modification with HF

S. SHIRAISHI*, K. KANAMURA and Z-I. TAKEHARA
Department of Energy and Hydrocarbon Chemistry, Graduate School of Engineering, Kyoto University, Yoshida-honmachi, Sakyo-ku, Kyoto 606-01, Japan
*(*author for correspondence, fax: +81 277 30 1353; present address: Department of Chemistry, Faculty of Engineering, Gunma University, Kiryu, Gunma 376-8515, Japan)*

Received 21 July 1998; accepted in revised form 19 January 1999

Key words: HF, lithium electrodes, surface modification, XPS measurements

Abstract

Surface modification of as-received lithium foils was carried out using acid-base reactions of the native surface films on lithium metal with HF. Two types of as-received lithium foils covered with different native films were used as samples for this surface modification. One was a lithium foil having a very thin native surface film and the other one had a thicker native surface film. The surface condition of the lithium metal was analysed by X-ray photoelectron spectroscopy before and after the surface modification using HF, and the coulombic efficiency was measured electrochemically. The thickness of the surface film on the modified lithium foils was related to the Li_2O layer thickness in the native film on the as-received lithium foils. The modified lithium foil which had the thinner native surface film provided more uniform deposition of lithium and a higher coulombic efficiency during charge and discharge cycles when propylene carbonate electrolyte with 1.0 M $LiPF_6$ was used as the electrolyte. These results show that the initial condition of the native surface film plays an important role in surface modification with HF.

1. Introduction

Electrodeposition of lithium metal is very important in the charging of rechargeable lithium metal batteries. This process has been investigated by many researchers in terms of the morphology of lithium which is a dominant factor in the rechargeability of lithium metal anodes [1–5]. Usually, the morphology of the lithium deposited in nonaqueous electrolytes has been found to be dendritic. The dendritic deposits are related to battery failure occurring during discharge and charge cycles [3, 4]. For example, dendritic lithium deposits can be easily detached from the current collector, so that they are electrically insulated from the current collectors. Such lithium metal becomes inactive and has been called 'dead lithium'.

The mechanism of electrodeposition of lithium has been discussed based on surface condition of lithium metal in nonaqueous electrolytes. The most popular model for the interface between lithium metal and nonaqueous electrolytes, proposed by Peled, is the solid electrolyte interface (SEI) model [6]. In this model, surface films formed on lithium metal can function as an ionically conductive interface, as well as a passivation film against undesirable reactions of lithium with the electrolyte. This means that the physical and chemical conditions of the SEI strongly affect the electrochemical behavior of lithium metal anodes. Therefore, many studies have been extensively performed to analyse surface films on lithium metal in nonaqueous electrolytes using various spectroscopic methods [7–29]. These studies have suggested that the morphology of lithium metal deposits depends on both chemical compositions and the three-dimensional structure of the surface films on lithium. The low physical and chemical uniformity of the surface film is related to the formation of the dendritic lithium. In order to obtain a high reversibility during dissolution and deposition cycles of lithium metal electrodes, the surface condition of lithium metal must be controlled. Recently, some researchers have

suggested various additives to the nonaqueous electrolytes for the surface modification of lithium metal, for example, CO_2 [30, 31], 2-Me furan [22, 32, 33], AlI_3 [22, 33], benzene [33], pyridine [34], and surfactants [35, 36]. We also found that a small amount of HF effectively reacts with various surface films on lithium metal to produce more suitable surface films which suppress the formation of the dendritic lithium. [37–39].

However, lithium metal foils are usually used as the anode of the rechargeable lithium battery. Especially, as-received lithium foil is important as a practical lithium anode. It is originally covered with surface films formed by chemical reactions of lithium metal with active gases (O_2, H_2O, CO_2 etc.) in the atmosphere during preparation or storage of lithium foils. Such surface films are called native film, consisting of various basic lithium compounds (Li_2CO_3, LiOH, and Li_2O). It is well known that such native films are undesirable SEI's in the sense of dendritic lithium formation [39, 40]. Therefore, the surface modification of as-received lithium foils is necessary to realize a highly reversible lithium metal anode for practical use.

On the one hand, the surface modification of as-received lithium foils can be carried out using additives. On the other hand, it can be easily predicted that the final surface condition of the lithium foils after the modification is strongly dependent on the original native surface film. However, there are no papers on the relationship between the condition of the native surface film and the effect of the surface modification with additives. In the case of the surface modification with HF, the influence of the initial condition of the native film on the final surface condition has not been discussed yet. Moreover, the modified surface film may show various morphologies of lithium deposits and different charge–discharge performance, depending on the initial native film. In this study, we used two types of as-received lithium foils having different surface conditions to clarify the dependence of the final condition of the surface film on the initial condition of the native surface films. Here, we first demonstrate that the chemical condition of the native film is extremely important in the subsequent surface modification process and the resulting electrochemical behavior.

2. Experimental details

2.1. *Lithium metal foil*

Two kinds of as-received lithium foils were used as samples for the surface modification. One (type A) was obtained from Honjo Metal Company (Japan) and had been kept under highly pure argon (dew point $< -80\ ^\circ C$) in a dry box for one month. Another (type B) was made from a lithium ingot under dry air and also had been kept under highly pure argon in a dry box for more than one year. These lithium foils were analysed with XPS before the surface modification to determine the chemical compositions the native surface films and to estimate their thickness. Both surface films on these lithium foils involved the same chemical species. However, the surface film on the type A lithium foil was thinner than that on the type B lithium foil.

2.2. *Surface modification with HF and electrochemical experiments*

The surface modification of the as-received lithium foils was performed through immersion of the lithium foils in propylene carbonate (PC) solution containing 1×10^{-3} mol dm^{-3} hydrogen fluoride (HF) for three days at room temperature. The preliminary experiments already confirmed that the modification reaction is sufficiently completed after the immersion for three days. The solution for the modification was prepared by addition of hydrofluoric acid (46 wt% aqueous solution, Wako Pure Chemical Industries, Ltd, Japan) into pure PC (Mitsubishi Chemical, Japan). After the surface modification, the lithium foils were washed with pure PC to quench the reactions between HF and the lithium foils.

Lithium metal was deposited on the modified lithium foils under galvanostatic conditions in PC containing 1.0 mol dm^{-3} $LiPF_6$ ($LiPF_6$/PC, Mitsubishi Chemical). The counter electrode was lithium foil (8 cm^2) and the reference electrode was Li/Li^+. The current density was set at 0.2 mA cm^{-2}, and the amount of electric charge was 1.0 C cm^{-2}.

Charge and discharge (deposition and dissolution) cycles under galvanostatic conditions were also performed to examine the surface condition changes of the modified lithium foils during such cycles. In this test, the charge process was carried out first following galvanostatic conditions. The current density was 2.0 mA cm^{-2}, and the amount of electric charge was 2.0 mA h cm^{-2} (7.2 C cm^{-2}). The discharge process was conducted under the same conditions as those for the first charge process.

After these electrochemical treatments, the lithium foils were washed with pure PC to remove electrolyte salts. All procedures were conducted in an argon dry box at room temperature (dew point $< -80\ ^\circ C$). The water contents of pure PC and electrolytes were estimated to be less than 20 ppm by analysis with a Karl Fischer Moisture Titrator (MKC-210, Kyoto Denshi Kogyo Co., Japan).

2.3. *XPS analysis and scanning electron microscopic (SEM) observations*

The samples were dried for 1 h under vacuum to remove residual PC on their surfaces. A transfer procedure for the samples from a dry box to the introduction chambers of the XPS and SEM instruments has been described in our previous paper [18]. The XPS analysis was performed by ESCA 850s (Shimadzu, Japan) under high vacuum conditions (less than 5×10^{-7} Pa). The Mg K_α line was used as an X-ray source (8 kV, 30 mA). The binding energy of each peak appearing in the XPS spectra was calibrated using that of elemental C in hydrocarbons, which was determined from the XPS spectra of C 1s for a hydrocarbon adsorbed on a standard silver sample. Argon ion etching (acceleration voltage, 2 keV; ion beam current, 8 μA) was applied to obtain depth profiles for elements involved in the surface films on lithium. The times in each figure indicate the argon etching duration. The etching rate is roughly estimated to be 5 Å min^{-1} from the sputtering coefficient and the actual ion beam current. An SEM observation of the morphology of lithium deposits on the lithium metal foils was performed using a JEM-25D (JEOL, Japan).

2.4. *XPS spectra of various lithium compounds as standard samples*

In general, decomposition of chemical compounds by X-ray radiation or Ar ion beam radiation is one of the serious problems in XPS depth analysis. Therefore, the damage to some lithium compounds, such as Li_2CO_3, LiOH, LiF, by X-ray radiation and Ar ion beam radiation was evaluated before the XPS analysis. Powders of these pure compounds were pelletized in a 6 mm diameter disc shape and then were exposed to X-ray radiation (8 kV, 30 mA) for 1 h or Ar ion beam (acceleration voltage, 2 kV; ion beam current, 8 μA) for 40 min in the XPS analysis chamber. LiF and Li_2CO_3 powders were purchased from Wako Chemical Industries, Ltd, and LiOH was synthesized by a vacuum drying treatment of LiOH–H_2O powder (Wako Pure Chemical Industries, Ltd, Japan) for 24 h at room temperature. Anhydrous LiOH was identified by an X-ray diffraction pattern in a dry atmosphere.

2.5. *Cycling test*

The reversibility of dissolution and deposition of lithium metal deposited on two types of lithium foils was tested under the following galvanostatic condition. The average percentage coulombic efficiency for many dissolution and deposition cycles was calculated according to Equation 4 [41]:

$$E_n = \frac{nQ_c}{nQ_c + Q_{ex}} \times 100 \quad (4)$$

where E is the average efficiency, Q_c is the amount of charge (deposition)/discharge (dissolution) electricity for each cycle, Q_{ex} the amount of electricity available from the lithium foil electrode (corresponding to excess lithium), and n are cycling numbers indicating an apparent 100% efficiency.

The percentage efficiency calculated by this equation corresponds to the ratio between the total amount of electricity for dissolution (nQ_c) and that for deposition (nQ_c) containing excess lithium (Q_{ex}). Therefore, the efficiency means the average coulombic utilization of deposited lithium on each cycle. The discharge was terminated at 1.0 V vs Li/Li^+. The type A and B lithium foils (80 μm thickness, 1 cm^2 area) were used as the lithium foil electrode. They were adhered onto a nickel plate which is the current collector. Because the volumetric energy density of lithium metal is 2061 mA h cm^{-3} [42], the amount of electricity of the lithium foil, Q_{ex}, is 16.5 mA h.

3. Results and discussion

3.1. *Influence of X-ray radiation and Ar ion beam radiation on lithium compounds*

Figure 1 shows the XPS spectra of Li 1s, O 1s, F 1s, and C 1s for LiF, LiOH, and Li_2CO_3 standard samples before and after X-ray radiation and Ar ion beam radiation (Ar ion etching). Two peaks were observed at 56.0 and 685.5 eV in the XPS spectra of Li 1s and F 1s for LiF (Figure 1 (a) and (b)), respectively, before either X-ray radiation or Ar ion beam radiation. These spectra were not changed by the X-ray radiation and the Ar ion beam radiation. Two peaks were observed (54.7 and 531.6 eV) in the XPS spectra of Li 1s and O1s for LiOH (Figure 1(c) and (d)), respectively. These peaks were not significantly changed by the X-ray radiation, although a slight decomposition of LiOH to Li_2O (at 53.7 eV in Li 1s and 528.8 eV in O 1s) was observed after Ar ion beam radiation for 20 min. However, no serious decomposition was observed after the consecutive Ar ion beam radiation. These spectra indicate that the influence of the Ar ion beam radiation on LiOH is not significant. Peaks were observed at 55.0, 532.0, and 290.2 eV in the XPS spectra of Li 1s and O 1s, and C 1s for Li_2CO_3 (Figure 1(e), (f) and (g)), respectively. A peak at

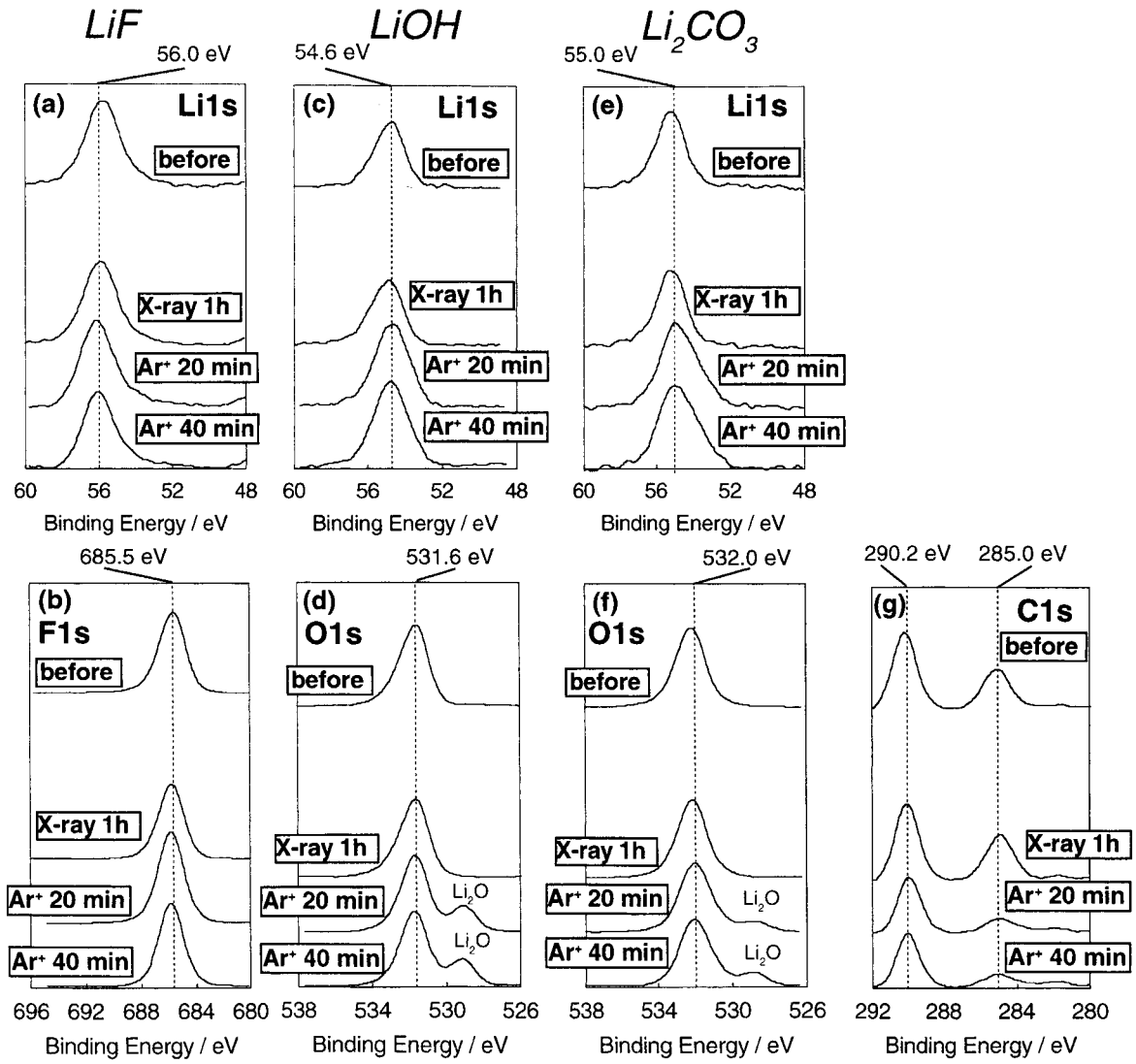

Fig. 1. XPS spectra of Li 1s, F 1s, O 1s, or C 1s for (a, b) LiF, (c, d) LiOH and (e, f) Li_2CO_3 standard samples before and after the X-ray radiation (8 kV, 30 mA) for 1 h and the Ar ion beam radiation (acceleration voltage; 2 kV, ion beam current; 8 μA) for 20 and 40 min.

285.0 eV in the C 1s spectra is due to a hydrocarbon gas adsorbed on the sample in the XPS analysis chamber. A slight decomposition of Li_2CO_3 to Li_2O was observed in the spectra after the Ar ion etching. This decomposition of Li_2CO_3 by the Ar ion beam radiation is negligible. From these results, it can be concluded that all compounds are sufficiently stable for the study of the surface chemical conditions of lithium foils from XPS depth profiles.

3.2. *Surface conditions of lithium metal foils*

Figures 2(a), (b), (c) and (d) show the XPS spectra of Li 1s, C 1s, O 1s, and their depth profiles for the type A lithium foil before the surface modification. These spectra were obtained after Ar ion etching for various durations. A peak at 55.0 eV in the Li 1s spectra before the Ar ion etching was attributed to Li_2CO_3, and another strong peak at 53.7 eV after the Ar ion etching for 5 min was attributed to Li_2O. The peak intensity changes of Li_2O and Li_2CO_3 in Figure 2(a) show the presence of Li_2O under a Li_2CO_3 layer. The peak corresponding to lithium metal was clearly observed after the Ar ion etching for 20 min, and the pattern of the Li 1s spectra was not changed by the subsequent Ar ion etching for 35–40 min. The peak of Li_2O was still observed after the Ar ion etching for 40 min. This may be due to reactions of lithium metal with residual H_2O

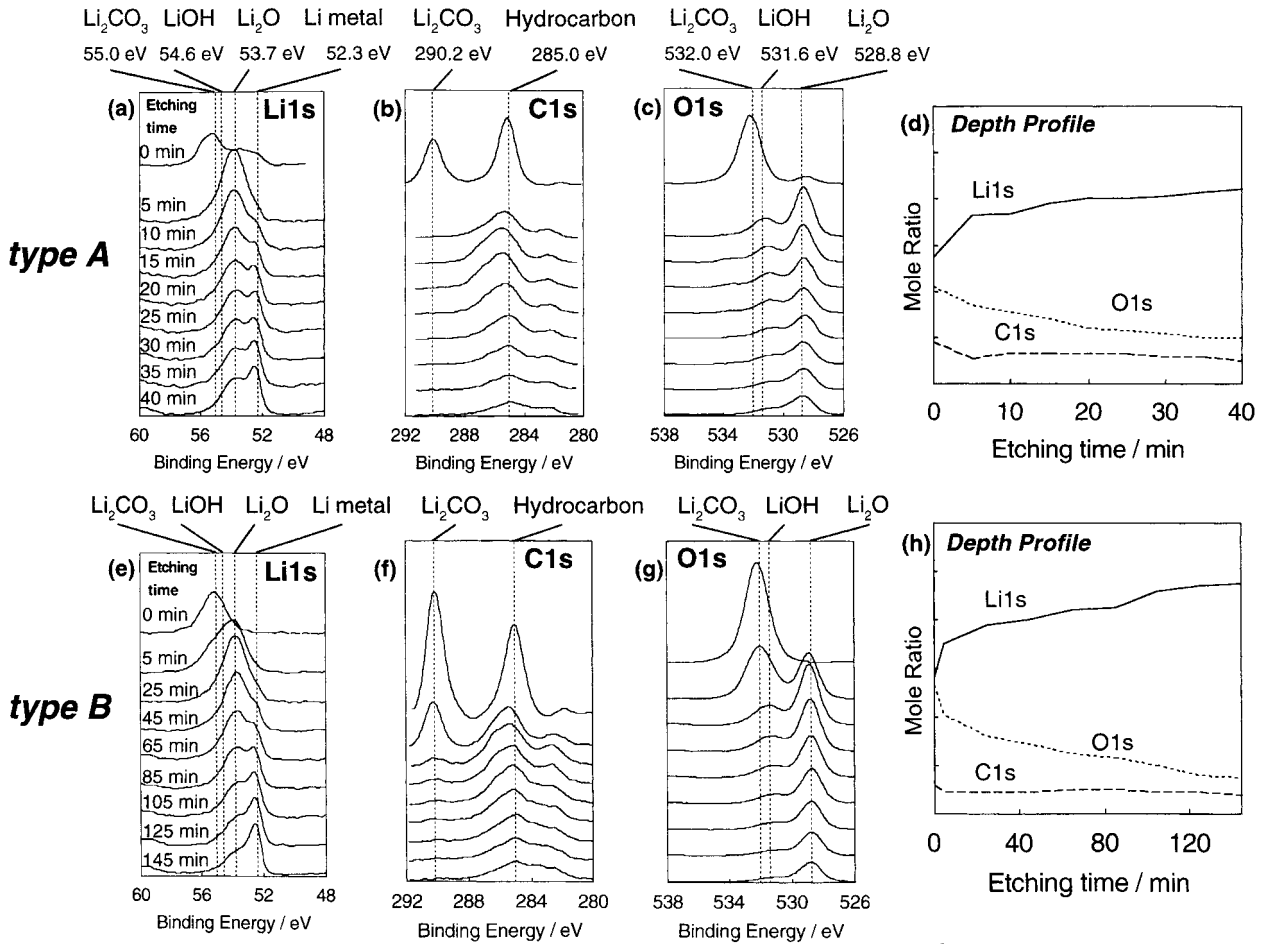

Fig. 2. XPS spectra of Li 1s, C 1s or O 1s and depth profiles of elements for (a–d) type A and (e–h) type B lithium foils before the surface modification. Time indicates the duration of the argon ion etching.

or O_2 in the XPS analysis chamber or to variation in the Ar ion beam radiation of lithium metal due to the surface roughness (distribution of the argon ion beam etching). In our previous study [43], we showed that the oxidation of lithium metal did not significantly occur in our XPS equipment within 1 h. Therefore, the observation of the Li_2O peak after Ar ion etching for 40 min may be mainly due to the surface roughness of this lithium foil. A peak of 290.2 eV, attributed to Li_2CO_3, however, disappeared on Ar ion etching. Therefore, it can be seen that Li_2CO_3 is present only at the outer part of the surface film on this lithium metal foil. A peak at 285.0 eV was attributed to hydrocarbon adsorbed on the lithium metal surface. Two peaks in the O 1s spectra before the Ar ion etching were observed at 532.0 and 528.8 eV, corresponding to Li_2CO_3 and Li_2O, respectively. After the Ar ion etching for 5 min, the peak of Li_2CO_3 disappeared, while a new peak at 531.7 eV attributed to LiOH was weakly observed. The peak of Li_2O was strongly observed after the Ar ion etching for 5 min, and its intensity gradually decreased during the Ar ion etching after 10 min duration. From these XPS spectra, it is concluded that the native film on the type A lithium foil consists of an outer layer involving Li_2CO_3/LiOH and an inner layer including Li_2O. From the peak corresponding to lithium metal, the surface film seems to be substantially removed by Ar ion etching for 40 min, indicating that the thickness of the surface film can be roughly estimated to be 200 Å (the thickness of the outer Li_2CO_3/LiOH layer is about 30 Å). From the XPS depth profiles, it is also confirmed that the amount of compounds involving oxygen such as Li_2CO_3 is greater at the outer layer of the surface film.

Figures 2(e), (f), (g) and (h) show the XPS spectra of Li 1s, C 1s, O 1s, and the XPS depth profile for the type B lithium foil before the surface modification. These spectra indicate that the surface film on the type B lithium foil consists of a Li_2CO_3/LiOH outer layer and a

Li_2O inner layer, which is similar to the type A lithium foil. The peak of lithium metal in the Li 1s spectra was first observed after Ar ion etching for 85 min, and the pattern of the Li 1s spectrum was not changed after Ar ion etching for 145 min. The peaks corresponding to Li_2CO_3 in the C 1 s and O 1s spectra diminished during Ar ion etching after 25 min duration. These results show that the surface film on the type B lithium foil is thicker than that on the type A lithium foil. Therefore, it can be said that the native film on the type B lithium foil is roughly 700 Å in thickness. The thickness of the outer Li_2CO_3/LiOH layer in the surface film may be 100 Å thickness.

3.3. *Surface condition of lithium metal modified by HF*

The surface modification of as-received lithium foils is essentially explained by acid-base reactions of HF with various basic lithium compounds in native surface films, as shown in Equations 1–3 [16, 17, 19, 39]:

$$Li_2CO_3 + 2\ HF \rightarrow 2\ LiF\ (\text{porous, weak}) + H_2CO_3 \quad (1)$$

$$LiOH + HF \rightarrow LiF\ (\text{porous, weak}) + H_2O \quad (2)$$

$$Li_2O + 2\ HF \rightarrow 2\ LiF\ (\text{dense, rigid}) + H_2O \quad (3)$$

These acid–base reactions indicate that a part of a native surface film, at least, is changed to a new surface film consisting of LiF. In previous papers [16, 17], we reported that the condition change of the surface film after the modification with HF is related to volume changes in the surface films induced by acid-base reactions with HF. The volume of lithium compounds per 1 mole of atomic lithium is shown in Table 1. The volume of Li_2CO_3 or LiOH is much larger that of LiF, and that of Li_2O is slightly smaller than that of LiF. Therefore, the volume of the surface film, involving a Li_2CO_3/LiOH layer, decreases through the acid-base reactions with HF and the volume of the Li_2O layer does not change significantly. This means that a porous LiF surface film is formed from the Li_2CO_3/LiOH layer and a dense and rigid LiF surface film is produced from the Li_2O layer.

Figures 3(a), (b), (c), (d) and (e) show the XPS spectra of Li 1s, C 1s, O 1s, F 1s and the XPS depth profile for the type A lithium foil after the surface modification with HF. A new peak observed at 56.0 eV in the Li 1s spectra before the Ar ion etching was attributed to LiF. This LiF peak intensity markedly decreased, and the peak at 53.7 eV attributed to Li_2O was strongly observed after Ar ion etching for 10 min. Finally, the peak corresponding to lithium metal became the main peak in the Li 1s spectra after Ar ion etching for 20 min. The Li 1s spectra did not significantly change during the Ar ion etching for 30∼40 min. Therefore, the thickness of the surface film after the modification may be estimated to be 150 Å. The peak attributed to Li_2CO_3 in the C 1s spectra was observed at 290.0 eV as observed before the modification. However, the intensity of the Li_2CO_3 peak was much weaker, compared with that before the modification, as shown in Figure 2(b). These spectra indicate that the amount of Li_2CO_3 in the surface film is decreased by the immersion in PC containing HF for three days. In the O 1s spectra, the peaks attributed to Li_2CO_3, LiOH and Li_2O were also observed at 532.0, 531.7, or 528.8 eV, respectively. The peak of LiF was observed at 685.5 eV in the XPS spectra of F 1s. The peak intensity became weak after the Ar ion etching, indicating that LiF was present at the outer part of the surface film. This result is in good agreement with the results obtained from the Li 1s spectra. Moreover, the amount of elemental F in the outer layer of the surface film was larger than those of elemental O and C, as shown in the XPS depth profile. From these results, it can be concluded that the native film on the type A lithium foil changes to the bilayer surface film consisting of LiF and Li_2O. This change is due to the acid–base reactions of basic lithium compounds with HF, as shown in Equations 1–3. LiF is a final product on the type A lithium foil immersed in PC containing a small amount of HF.

Figures 3(f), (g), (h), (i) and (j) show the XPS spectra of Li 1s, C 1s, O 1s, F 1s, and the XPS depth profile for the type B lithium foil after the surface modification with HF. These spectra also indicate that the native surface film on the type B lithium foil changed to the bilayer consisting of LiF and Li_2O through the surface modification with HF. However, the thickness of the modified surface film on the type B lithium foil was greater than that of the type A lithium foil. The spectra of Li 1s was not changed by the Ar ion etching for 125 ∼145 min, indicating that the surface film was

Table 1. Volume of lithium and lithium compounds per 1 mole lithium atom

Compounds	Molar volume /cm^3	Volume per 1 mole lithium atom/cm^3
Li_2CO_3	35.2	17.6
LiOH	16.4	16.4
$LiOH.H_2O$	27.8	27.8
LiF	9.84	9.84
Li_2O	14.8	7.42
Lithium metal	13.0	13.0

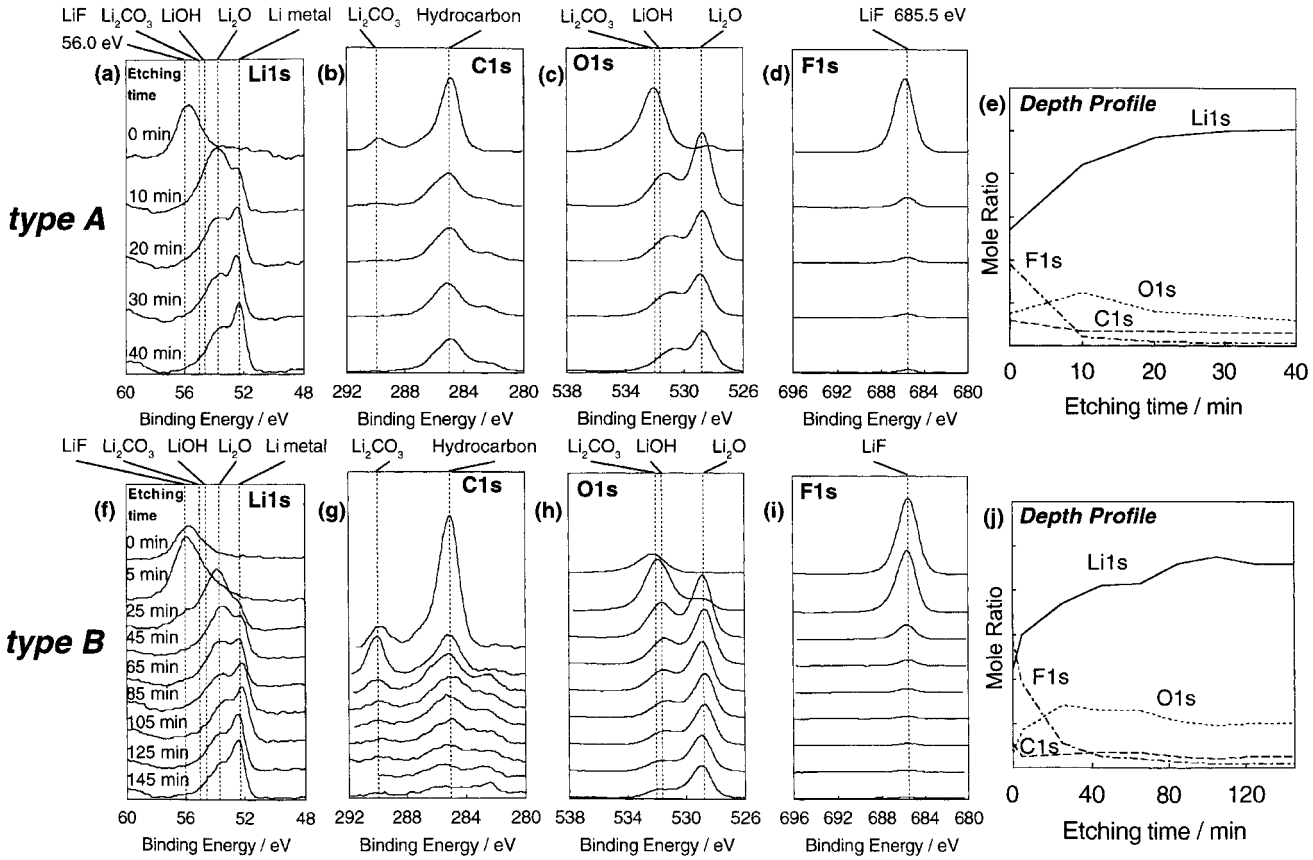

Fig. 3. XPS spectra of Li 1s, C 1s, O 1s or F 1s and depth profiles of elements for (a–e) type A or (f–j) type B lithium foils after the surface modification. The surface modification is conducted by the immersion of the lithium foils in PC containing 1×10^{-3} mol dm^{-3} HF for three days. Time indicates the duration of the argon ion etching.

substantially removed by Ar ion etching for 125 min. Therefore, the thickness can be roughly estimated to be 600 Å. These results indicate that the structure of the modified surface film is strongly affected by the condition of the original surface film before the modification. As shown in the Li 1s spectra in Figure 2(a,e) and Figure 3(a,f), the decrease in the thickness of the surface film on the type B lithium foil was about 100 Å, while the decrease on the type A lithium foil was about 50 Å.

The surface conditions of the two type of lithium foils before and after the modification with HF are schematically illustrated in Figure 4. The decrease in the thickness of the surface film caused by the modification was larger for type B than that for type A. The decrease in the film thickness seems to be related to the amount (thickness) of Li_2CO_3 or LiOH in the native film before the modification. Therefore, considering the above results by XPS and the modification reaction as shown in Equations 1–3, the decrease in the surface film, namely, the etching of the surface film is explained by removal of the porous and weak LiF layer produced from the Li_2CO_3/LiOH layer (in our previous paper, such a removal of a part of the native film has already been identified by the *in situ* FTIR spectroscopy [44]). The etching is terminated by the formation of the LiF layer, produced from the Li_2O layer, because of the high rigidity and stability of the LiF layer. Therefore, it can be said that the thickness of the surface film modified with HF is determined by the thickness of Li_2O layer in the initial native film.

3.4. *Electrodeposition of lithium on lithium metal foil*

The electrodeposition on the modified or untreated lithium foils (the type A or B lithium foils) was performed under galvanostatic condition (0.2 mA cm^{-2}, 1.0 C cm^{-2}) in 1.0 mol dm^{-3} $LiPF_6$/PC, and then the morphology of lithium deposited on the lithium foils was observed. Figure 5 shows the scanning electron micrographs of these lithium deposits. From (a), (b), (e) and (f), it is found that dendritic lithium is formed on

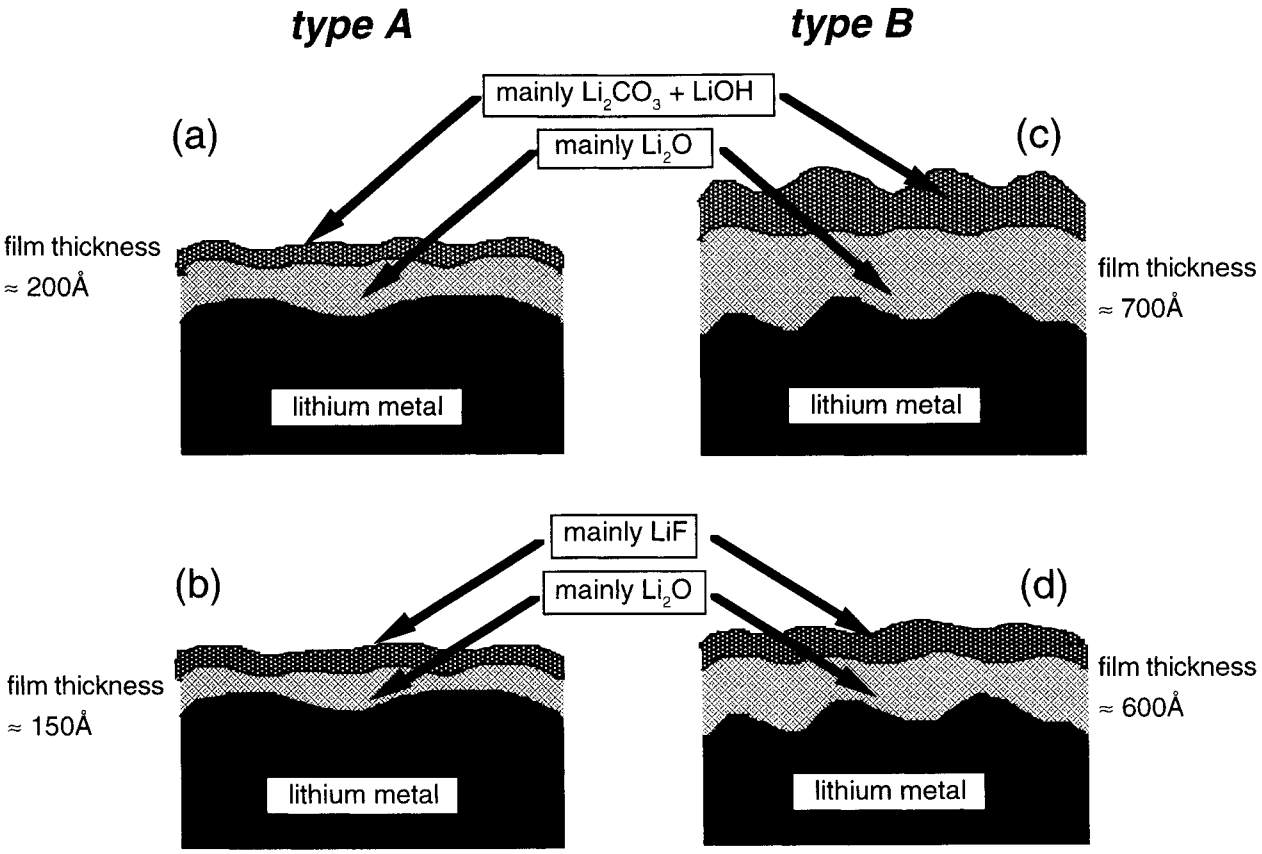

Fig. 4. Schematic illustration of the surface films formed on the lithium foils before and after the surface modification with HF. The surface modification of lithium metal was performed by the immersion of the lithium foils in PC containing 1×10^{-3} mol dm^{-3} HF for three days. Key: (a) type A before modification, (b) type A after modification, (c) type B before modification and (d) type B after modification.

both of the unmodified lithium metal foils. This result indicates that the surface films on the as-received lithium foils promote the lithium dendrite formation in 1.0 M $LiPF_6$/PC. On the other hand, spherical particles were obtained by the electrodeposition in 1.0 mol dm^{-3} $LiPF_6$/PC when the deposition of lithium was carried out on the lithium modified with HF, as shown in (c), (d), (g) and (h). The SEM observation indicates that the surface modification with HF is effective in suppressing the lithium dendrite formation on the lithium foils.

The morphology of electrochemically deposited particles is strongly affected by the current distribution on the substrate. When a lithium foil is used as a substrate, the current distribution is influenced by not only standard electrochemical factors but also the physical and chemical conditions of the surface film on the lithium foil. If an electrodeposition current is concentrated at specific points on the surface film at which the resistivity is low (a high ionic conductivity), dendrite deposition is promoted. The modified surface film on the lithium foils used in this study did not produced dendrites. This fact can be explained by the formation of uniform surface films on the lithium foils through the HF treatment [39]. However, the morphologies of lithium deposits on modified lithium foils of type A and type B were different as shown in Figures 5(c), (d), (g) and (h). Lithium particles were more locally deposited on the modified type B lithium foil compared with the electrodeposition on the type A lithium foil. This result indicates that the nonuniformity of the surface film on the modified type B lithium foil is still present resulting in patches of deposits. Consequently, the surface condition of lithium foils before the HF surface modification is also very important.

3.5. *Surface condition of modified lithium metal foil after charge and discharge cycles*

Figure 6 shows the scanning electron micrographs of the modified type A lithium foil after charge and discharge cycles. The charge and discharge current densities were set at 2.0 mA cm^{-2}, and the capacity

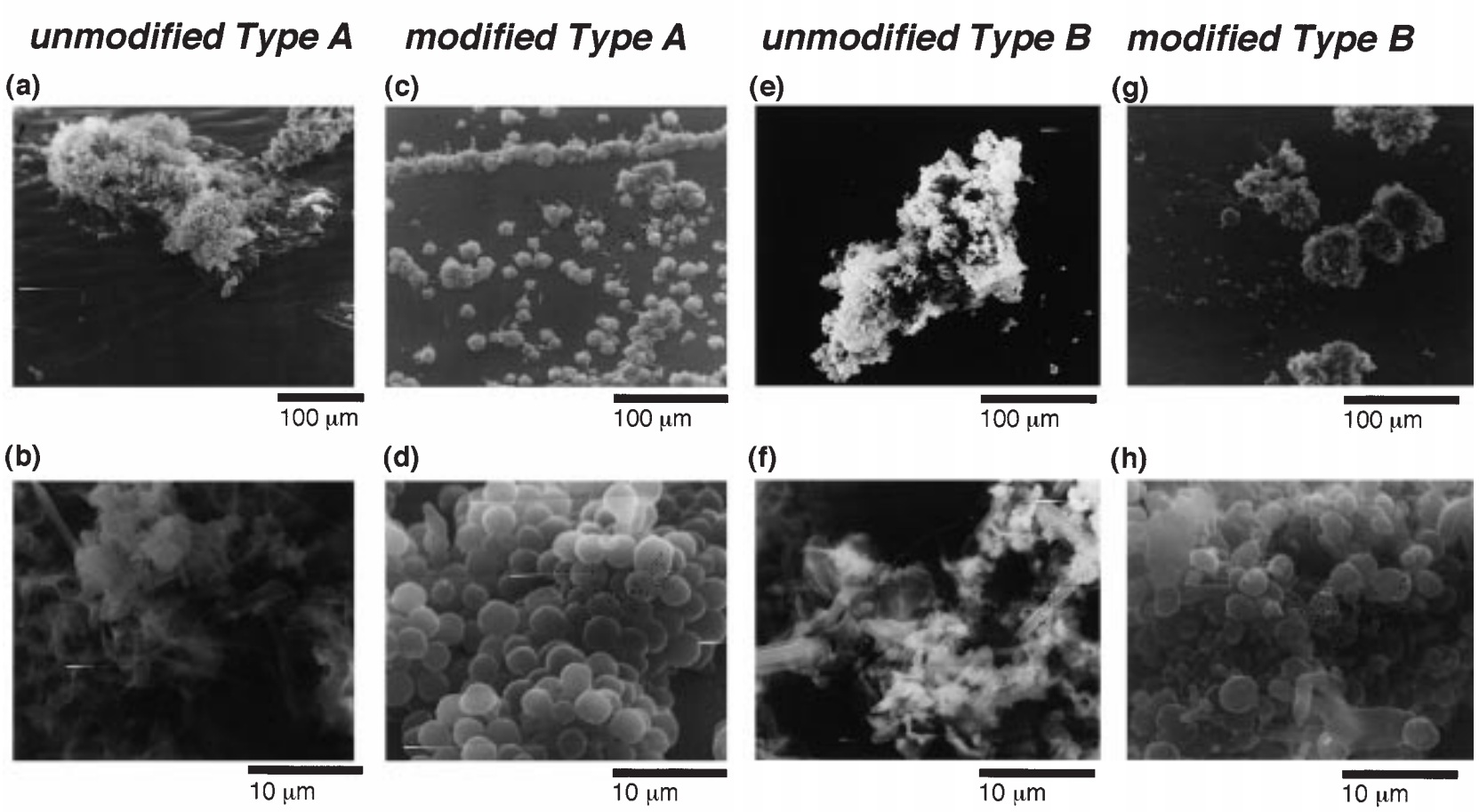

Fig. 5. Scanning electron micrographs for lithium electrodeposited (0.2 mA cm^{-2}, 1.0 C cm^{-2}, in 1.0 mol dm^{-3} $LiPF_6$/PC) on the type A (a–d) or type B (e–h) lithium foil before or after the surface modification with HF.

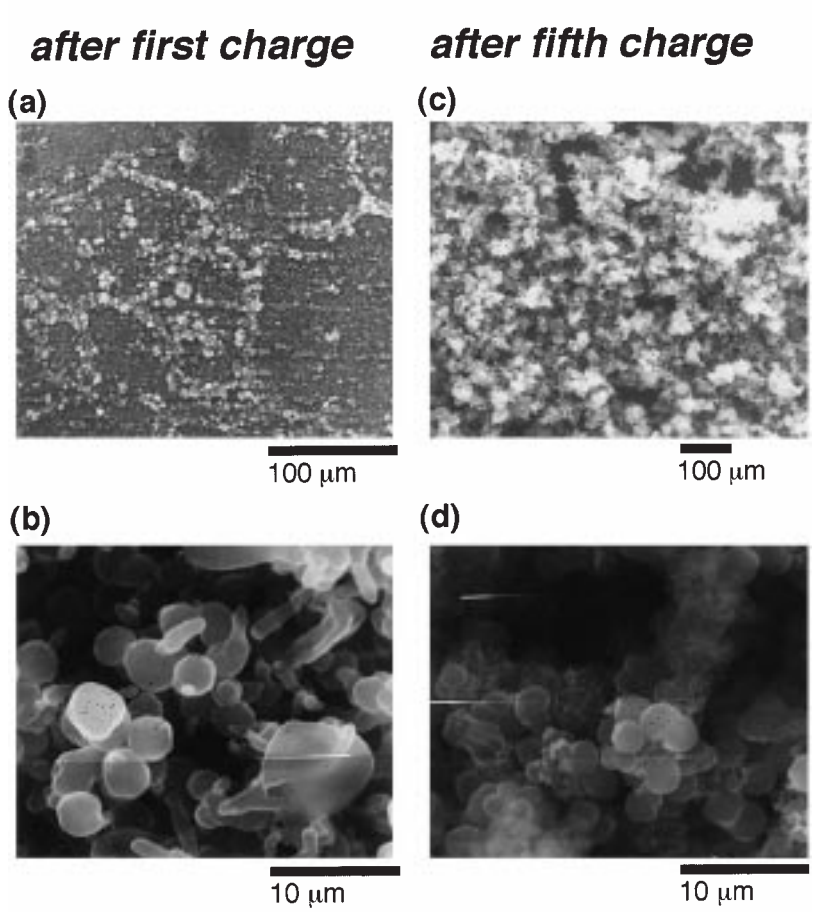

Fig. 6. Scanning electron micrographs for the type A lithium foil modified with HF after several discharge (dissolution) and charge (deposition) cycles under galvanostatic condition in 1.0 mol dm^{-3} $LiPF_6$/PC. Current density was set at 2.0 mA cm^{-2}, amount of electricity for cycles were set at 2.0 mA h cm^{-2}. Key: (a, b) after the first charge, and (c, d) after the fifth charge.

was set at 2.0 mA h cm^{-2}. Spherical particles were observed after the charge and discharge cycle. Figures 7(a), (b), (c), (d) and (e) show the XPS spectra of Li 1s, C 1s, O 1s, F 1s, and the XPS depth profile for the modified type A lithium foil after the first charge. Because the lithium foil was mostly covered with the lithium particles shown in Figure 6, the XPS spectra in Figures 7(a), (b), (c), (d) and (e) mainly reflect the surface film on the lithium deposits. All XPS spectra of Li 1s, C 1s, O 1s, and F 1s resembled those of the modified lithium foil before the first charge, as shown in Figures 3(a), (b), (c) and (d). No peaks were observed in the XPS spectra of P 2p. This indicates that no compounds involving elemental phosphorus are present in the surface film on the lithium deposits. From these results, it can be said that the surface film on the lithium deposits also consists of the bilayer structure consisting of LiF and Li_2O. The formation of this surface film is partly due to the presence of a small amount of HF in $LiPF_6$/PC. It is known that 1.0 M $LiPF_6$/PC electrolyte contains a small amount of HF because of the hydrolysis of $LiPF_6$ [45]. In previous work [39], when using electrolyte not containing HF such as 1.0 mol dm^{-3} $LiClO_4$/PC, even though the surface film on the lithium metal foil was modified by HF, lithium dendrites formed during electrodeposition, indicating that the presence of HF in an electrolyte is necessary for a smooth electrodeposition on lithium metal. Therefore, both the surface films on the lithium foils and the surface films of the lithium deposits must consist of the LiF/Li_2O bilayer surface film for the smooth lithium deposition.

Figures 7(f), (g), (h), (i) and (j) show the XPS spectra of Li 1s, C 1s, O 1s, and F 1s and the XPS depth profile for the modified type A lithium foil after the fifth charge. These XPS spectra were slightly different from those after the first charge. In the Li 1s spectra, the peak from

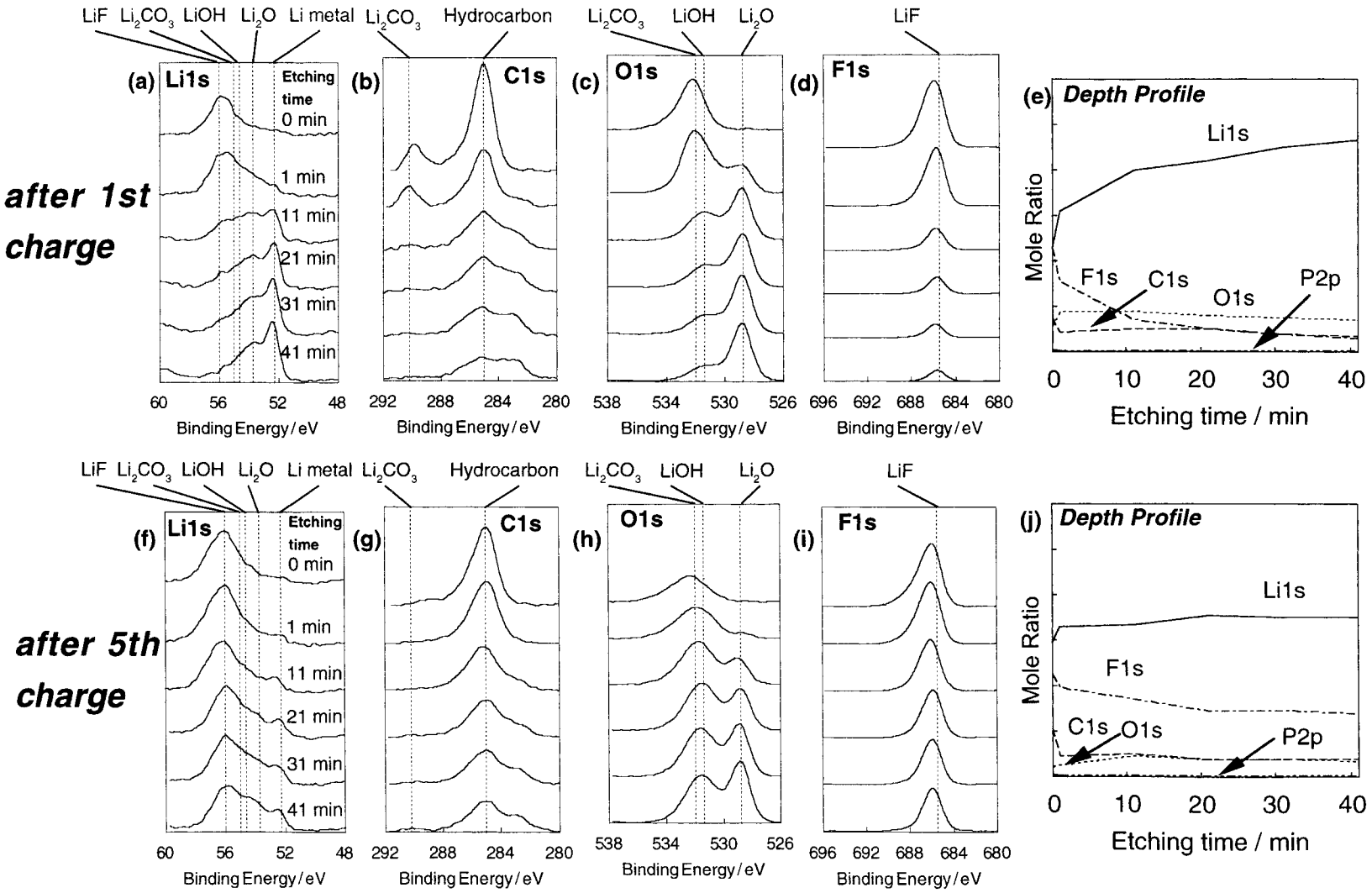

Fig. 7. XPS spectra of Li 1s, C 1s, O 1s, or F 1s and the depth profiles for the type A lithium foil modified with HF after several discharge and charge cycles under galvanostatic condition in 1.0 mol dm^{-3} $LiPF_6$/PC. Current density was set at 2.0 mA cm^{-2}, amount of electricity for cycle was set at 2 mA h cm^{-2}. Key: (a–e) after the first charge, and (f–j) after the fifth charge.

lithium metal was weak, even after Ar ion etching for 11 min. The peak of Li_2CO_3 was not observed in the C 1s spectra before or after Ar ion etching. The peak of LiF was not changed by Ar ion etching. These XPS spectral features show that the surface film on the lithium deposits after the fifth charge was thicker than that after the first charge. The amount of elemental F was large even after Ar ion etching as shown in the depth profile. From these results, it is concluded that this thick surface film is the LiF layer. Possibly, the formation of such a thick LiF layer is due to accumulation of thin LiF surface films left on the substrate electrode by the discharge (dissolution) process of lithium deposits on lithium metal.

3.6. *Cycling test*

Table 2 shows the average cycle efficiency of the lithium foil anodes in 1.0 mol dm^{-3} $LiPF_6$/PC. The efficiency of the type A lithium foil modified with HF was higher than that of the type B lithium foil modified with HF or the unmodified lithium foils. The improvement in cycle efficiency is due to the suppression of dendrite formation by the surface modification. The efficiency under the discharge and charge cycle conditions of low current density and small electric charge was higher than that for high current density and large electric charge. Because the shapes of the lithium deposits at low current density and small charge were more uniform than those at high current density and large charge, as shown in Figure 5 (c,d) and Figure 6 (a,b), the differences in the cycle efficiency may be related to the differences in the shape of the deposits. The uniform shape of the deposits may be advantageous for efficient discharge and charge cycles. However, even when such spherical particles are deposited, the efficiency is not 100%. This suggests that even the spherical particles may cause some dead lithium or consumption of lithium metal by reactions with the electrolytes.

Table 2. Average cycle efficiency for lithium metal

Lithium	Current density, Q_c^*	Efficiency/%
Unmodified (type A)	2.0 mA cm^{-2}, 2.0 mA h cm^{-2}	67
Unmodified (type B)	2.0 mA cm^{-2}, 2.0 mA h cm^{-2}	53
Modified† (type A)	2.0 mA cm^{-2}, 2.0 mA h cm^{-2}	80
Modified† (type B)	2.0 mA cm^{-2}, 2.0 mA h cm^{-2}	70
Modified† (type A)	0.2 mA cm^{-2}, 0.2 mA h cm^{-2}	92

* Amount of discharge and charge electricity for each cycle
† Modification is the immersion in PC containing 1×10^{-3} mol dm^{-3} HF for three days

4. Conclusions

Two kinds of as-received lithium foils having different native films were used as samples for the surface modification with propylene carbonate solution containing a small amount of HF. These native films consisting of a Li_2CO_3/LiOH layer and a Li_2O layer were changed to a LiF/Li_2O bilayer, and the thickness in the film was decreased by the surface modification. However, the final conditions were different in these two lithium foils. The following remarks are based on our surface analyses:

(i) The decrease in the thickness of the surface film by the HF treatment is related to the thickness of the Li_2CO_3/LiOH layer in the native film.
(ii) The thickness of the final surface film after the modification with HF is determined by the thickness of the Li_2O layer in the native film.

These final surface conditions of the lithium foils influence the morphology and the distribution of lithium deposits. Moreover, the discharge and charge characteristics as anodes in rechargeable lithium batteries also depended on the final conditions of the lithium foils. When the lithium foil having a thinner native surface film was modified with HF, the dendrite formation was more effectively suppressed during several discharge and charge cycles, and the average cycle efficiency was more improved. This result indicates that the condition of the initial native film affects the uniformity of the surface film after the surface modification with HF.

Acknowledgement

This work was supported by grant-in-aid for scientific research (no. 07555575) from the Japanese Ministry of Education, Science and Culture.

References

1. J.P. Gabano, in J.P. Gabano (ed.) *Lithium Batteries*, Academic Press, London, 1983, chapter 2.
2. V.R. Koch, *J. Power Sources* **6** (1981) 357.
3. I. Yoshimatsu, T. Harai and J. Yamaki, *J. Electrochem. Soc.* **135** (1988) 2422.
4. M. Arakawa, S. Tobishima, Y. Nemoto, M. Ichimura and J. Yamaki, *J. Power Sources* **43–44** (1993) 27–35.
5. R. Selim and P. Bro, *J. Electrochem. Soc.* **121** (1974) 1457.

6. E. Peled, *J. Electrochem. Soc.* **126** (1979) 2047.
7. D. Aurbach, M.L. Daroux, P.W. Faguy and E. Yeager, *J. Electrochem. Soc.* **134** (1987) 1611.
8. D. Aurbach and O. Chusid, *J. Electrochem. Soc.* **140** (1993) L1.
9. D. Aurbach, A. Zaban, A. Schechter, Y. Ein-Eli, E. Zinigrad and B. Markovsky, *J. Electrochem. Soc.* **142** (1995) 2873.
10. D. Aurbach and E. Granot, *Electrochim. Acta* **42** (1997) 697.
11. M. Odziemkowski, M. Krell and D.E. Irish, *J. Electrochem. Soc.* **139** (1992) 3052.
12. K. Wang, G.S. Chottiner and D.A. Scherson, *J. Phys. Chem.* **97** (1993) 11075.
13. K. Wang, P.N. Ross, Jr., F. Kong and F. McLarnon, *J. Electrochem. Soc.* **143** (1996) 422.
14. S.P.S. Yen, D. Shen, R.P. Vasquez, F.J. Grunthaner and R.B. Somoano, *J. Electrochem. Soc.* **128** (1981) 1434.
15. K.R. Zavadil and N.R. Armstrong, *Surfa. Sci.* **230** (1990) 47.
16. K. Kanamura, H. Tamura and Z. Takehara, *J. Electroanal. Chem.* **333** (1992) 127.
17. K. Kanamura, S. Shiraishi, H. Tamura and Z. Takehara, *J. Electrochem. Soc.* **141** (1994) 2379.
18. K. Kanamura, H. Tamura, S. Shiraishi and Z. Takehara, *J. Electroanal. Chem.* **394** (1995) 49.
19. K. Kanamura, H. Tamura, S. Shiraishi and Z. Takehara, *Electrochim. Acta* **40** (1995) 913.
20. D. Aurbach, I. Weissman, A. Schechter and H. Cohen, *Langmuir*, **12** (1996) 3991.
21. K. Naoi, M. Mori and Y. Shinagawa, *J. Electrochem. Soc.* **143** (1996) 2517.
22. M. Ishikawa, S. Yoshitake, M. Morita and Y. Matsuda, *J. Electrochem. Soc.* **141** (1994) L159.
23. N. Koura, S. Tamura and M. Yoshitake, *Denki Kagaku*, **63** (1995) 623.
24. D. Aurbach and Y. Cohen, *J. Electrochem. Soc.* **143** (1997) 3525.
25. Y. Geronov, F. Schwager and R.H. Muller, *J. Electrochem. Soc.* **129** (1982) 1422.
26. J.G. Thevenin and R.H. Muller, *J. Electrochem. Soc.* **134** (1987) 273.
27. D. Aurbach and A. Zaban, *J. Electroanal. Chem.* **348** (1993) 155.
28. M. Odziemkowski and D.E. Irish, *J. Electrochem. Soc.* **140** (1993) 1546.
29. D. Pletcher, J.F. Rohan and A.G. Ritchie, *Electrochim. Acta* **39** (1994) 2015.
30. D. Aurbach, Y. Gofer, M. Ben-Zion and P. Aped, *J. Electroanal. Chem.* **339** (1992) 451.
31. T. Osaka, T. Momma, T. Tajima and Y. Matsumoto, *J. Electrochem. Soc.* **142** (1995) 1057.
32. K.M. Abraham, J.S. Foos and J.L. Goldman, *J. Electrochem. Soc.* **131** (1984) 2197.
33. M. Morita, S. Aoki and Y. Matsuda, *Electrochim. Acta* **37** (1992) 119.
34. H. Nakamura, C. Wang, E. Mitani, T. Fujita and M. Yoshio, *J. Surf. Finish. Soc. Jpn.* **46** (1995) 1187.
35. T. Hirai, I. Yoshimatsu and J. Yamaki, *J. Electrochem. Soc.* **141** (1994) 2300.
36. A.T. Ribes, P. Beaunier, P. Willmann and D. Lemordant, *J. Power Sources* **58** (1996) 189.
37. K. Kanamura, S. Shiraishi and Z. Takehara, *J. Electrochem. Soc.* **141** (1994) L108.
38. K. Kanamura, S. Shiraishi and Z. Takehara, *J. Electrochem. Soc.* **143** (1996) 2187 .
39. S. Shiraishi, K. Kanamura and Z. Takehara, *J. Appl Electrochem.* **25** (1995) 584.
40. T. Fujieda, N. Yamamoto, K. Saito, T. Ishibashi, M. Honjo, S. Koike, N. Wakabayashi and S. Higuchi, *J. Power Sources* **52** (1994) 197.
41. T. Osaka, T. Momma, K. Nishimura and T. Tajima, *J. Electrochem. Soc.* **140** (1993) 2745.
42. D. Fauteux and R. Koksbang, *J. Applied. Electrochem.* **23** (1993) 1.
43. K. Kanamura, S. Shiraishi, H. Takezawa and Z. Takehara, *Chem. Mater.* **9** (1997) 1797.
44. K. Kanamura, H. Takezawa, S. Shiraishi and Z. Takehara, *J. Electrochem. Soc.* **144** (1997) 1900.
44. D.W.A. Sharp, in M. Stacey, J.C. Tatlow and A.G. Sharpe (ed.), *Advances in Fluorine Chemistry*, vol. 1, Butterworths, London, 1960, p. 69.